Journal of Orthopaedic Translation (2019) 18, 40—47

Available online at www.sciencedirect.com

ScienceDirect

journal homepage: http://ees.elsevier.com/jot

ORIGINAL ARTICLE

A novel method for estimating nail-tract bone density for intertrochanteric fractures

Rui Zhang [a,1], Ling Wang [c,1], Yanyu Lin [a,b], Minghui Yang [d], Zhe Guo [c], Wei Xia [a], Jie Wei [d], Chen Yi [d], Xinbao Wu [d], Xiaoguang Cheng [c,], Xin Gao [a,*]**

[a] *Medical Imaging Department, Suzhou Institute of Biomedical Engineering and Technology, Chinese Academy of Sciences, Suzhou, China*
[b] *College of Materials Sciences and Opto-Electronic Technology, University of Chinese Academy of Sciences, Beijing, China*
[c] *Department of Radiology, Beijing Jishuitan Hospital, Peking University Fourth School of Clinical Medicine, Beijing, China*
[d] *Department of Traumatology and Orthopedic Surgery, Beijing Jishuitan Hospital, Peking University Fourth School of Clinical Medicine, Beijing, China*

Received 4 May 2018; received in revised form 29 September 2018; accepted 28 November 2018
Available online 21 December 2018

KEYWORDS
Fracture;
Intramedullary nails;
Nail tract;
Proximal femur;
Volumetric bone mineral density

Abstract *Summary:* A novel method based on voxel-based morphometry was proposed to investigate the average volumetric bone mineral density (vBMD) of femoral head nail tract in patients treated with intramedullary nails—proximal femoral nail antirotation (PFNA) and gamma nail (GN). The results showed that there was no significant difference in average vBMD between the two groups.

Background: For unstable intertrochanteric fractures, poor bone quality might be one of the most important causes of cut-out complications in the femoral head during surgical treatment. Bone quality is generally regarded as an equivalent of BMD. Thus, we develop a novel voxel-based morphometry—based method to quantify vBMD of the femoral head nail tract.

Methods: Automatic calculation of average vBMD of nail tracts requires three main steps. First, we built a standard nail tract in a proximal femur template. Then, we mapped the proximal femur structure of each patient to the template by B-spline and Demons registration so that the anatomical positions of the proximal femur of all patients spatially corresponded to the standard template. Finally, we calculated and visualized the average vBMD

* Corresponding author. No. 88 Keling Road, Suzhou New District, Suzhou 215163, Jiangsu, China.
** Corresponding author. No. 31 East Xinjiekou Street, Xicheng District, Beijing 100035, Beijing, China.
E-mail addresses: ruizhang724@163.com (R. Zhang), doctorwl@bjmu.edu.cn (L. Wang), linyanyu15@gmail.com (Y. Lin), doctyang0125@126.com (M. Yang), guoz1982@163.com (Z. Guo), xiav1990@163.com (W. Xia), jie_wei1212@163.com (J. Wei), ashelian@126.com (C. Yi), xinbao_wu@126.com (X. Wu), xiao65@263.net (X. Cheng), xingaosam@yahoo.com (X. Gao).
[1] Rui Zhang and Ling Wang are primary authors and contributed equally. Xiaoguang Cheng and Xin Gao are the joint corresponding authors.

https://doi.org/10.1016/j.jot.2018.11.005

distribution of the nail tract of all patients. To verify the feasibility of the method, we enrolled 75 patients (52 women and 23 men) with hip fractures to our study to compare measurements. The root mean square of the standard deviation (RMSSD) was calculated, and the coefficient of variation (CV) of the RMSSD (CV-RMSSD) was used to evaluate the reproducibility of intraoperator and interscan measurements. The Mann—Whitney U test was used to compare the average vBMD of nail tracts for the PFNA and GN.
Results: The CV-RMSSD of intraoperator measurements ranged from 1.0% to 2.0%, and the CV-RMSSD of interscan measurements ranged from 3.6% to 4.5%. There was no significant difference in the average vBMD between patients with PFNAs and those with GNs ($p > 0.05$).
Conclusions: The proposed method is reproducible for determining the average vBMD, which may provide a reference index for selection of appropriate intramedullary nails for individual patients. The current choice of intramedullary nail based on the experience of a surgeon may be biased.
The translational potential of this article: A novel method was proposed to measure the spatial average vBMD of nail tracts, which has good potential to provide a reference index for surgeons to choose appropriate implants.

Introduction

With ageing, the prevalence and incidence of osteoporotic hip fractures increase significantly [1]. Intertrochanteric fracture, a major anatomy-based type of hip fracture, has a relatively high mortality [2,3]. Early surgical treatment is the preferred choice because it might allow early full weight-bearing and rehabilitation. However, the major implant failure in the fixation of intertrochanteric treatment is cut-out defined as "the collapse of the neck-shaft angle into varus, leading to extrusion of the screw from the femoral head", with the incidence of 3—15% [4]. Most hip fracture treatment studies mainly focused on surgical methods and types of intramedullary nails to minimize the risk of failure [2,5]. Intramedullary nails were widely used in the treatment of intertrochanteric fractures, and there are two main types: the proximal femoral nail antirotation (PFNA; DePuy Synthes, Raynham, MA, USA) and the gamma nail (GN; Stryker, Kalamazoo, MI, USA) [5,6]. The lag screw of the GN can exert more compression at the fracture site, which requires good femoral head bone quality to provide sufficient grip force. In comparison, inserting the PFNA blade compacts the cancellous bone, providing additional anchoring, which is more suitable for osteoporotic patients with severe bone loss of the femoral head. Except the insertion of suitable implants, poor bone quality might be one of the important causes of cut-out complications [7]. In the implant literature, bone quality is generally considered to be an equivalent of bone mineral density (BMD) [8]. BMD measurements of the nail tract might have promise as a reference index to be used by treating surgeons.

Dual X-ray absorptiometry (DXA) is widely used for the measurement of BMD [9], but it is limited by its two-dimensional methodology. Quantitative computed tomography (QCT) can measure volumetric bone mineral density (vBMD) derived from three-dimensional imaging [10,11]. Since 2009, methods such as voxel-based morphometry (VBM) for the spatial assessment of vBMD from QCT images have been validated and successfully applied in hip fracture studies. VBM is a computational technique that has been used to analyze statistical differences between groups of magnetic resonance brain images. Compared with the conventional region of interest analysis, VBM is fully automated and unbiased and is not restricted to the analysis of specific regions. Therefore, VBM has been widely used in hip fracture studies in recent years [12—17]. However, these methods cannot measure the BMD of the femoral head nail tract. Thus, there is little known about the relationship of BMD to the selection of intramedullary nail type. If a standard method for measuring the BMD distribution of the nail tract using QCT can be developed, it may be possible to identify what type of nail is best for specific patients.

The purpose of our study was to: (1) develop a novel VBM-based method to estimate and display the vBMD of the femoral head nail tract; (2) validate the intraoperator and interscan reliability of this method for measuring vBMD distribution of the femoral head nail tract; and (3) compare the differences in vBMD of the femoral head nail tract between the PFNA and GN.

Materials and methods

Patients

Seventy-five patients (52 women and 23 men) with hip fractures (49 patients with intertrochanteric fractures and 26 with femoral neck fractures) were enrolled from the radiology department within the emergency department of Beijing Jishuitan Hospital at some point between January 2015 and December 2016. The enrolment process for our study was as described by Yu et al [17]. For patients with hip fracture, all the cases were acute trauma, and the

contralateral proximal femur was analyzed. Because of concerns about radiation dose, we did not require patients to have two computed tomography (CT) scans to assess interscan precision; however, patients with a femoral neck fracture who needed cannulated screw fixation were recruited for interscan cases because they had two hip CT scans, once before and once after surgery. Those patients underwent a second scan to confirm implant position. The study inclusion criteria also specified that implant fixation artifacts would not affect the quality of images of the contralateral hip (Figure 1) and that the two hip scans had to be obtained within 72 h interval to minimize changes in BMD caused by hip fractures [18]. Finally, the preoperative and postoperative CT scans of 26 patients were used for the assessment of interscan precision. For the intraoperator group, 29 patients were randomly selected from the 75 cases to meet conservative recommendations (>27 degrees of freedom) for estimation of reproducibility error [19]. The preoperative CT scans of 49 patients with low-energy intertrochanteric fractures (33 with GNs and 16 with PFNAs) were used to compare the nail tract BMD of two different types of intramedullary nails. The choice of PFNA or GN in unstable intertrochanteric fractures is based on the experience of a surgeon. Proof of informed consent was obtained from all study participants. Study protocol was approved by the Ethics Committee of Beijing Jishuitan Hospital, and all methods were performed in accordance with approved guidelines.

Image acquisition

Bilateral hip QCT data were obtained using a Toshiba Aquilion 16-slice CT scanner (Toshiba Medical Systems Corporation, Tokyo, Japan) in the emergency department with a calibration phantom (Mindways Software Inc., Austin, TX, USA) beneath the hip. With the software available on the CT scanner console, a calibration phantom in a QCT procedure is experimentally used to obtain a calibration curve in which the Hounsfield units (HUs) are converted to corresponding BMD values. The following CT acquisition parameters were used: 120 kVp, 125 mA, 1-mm slice thickness, 50-cm field of view and a matrix size of 512 × 512 pixels in spiral and standard reconstructions.

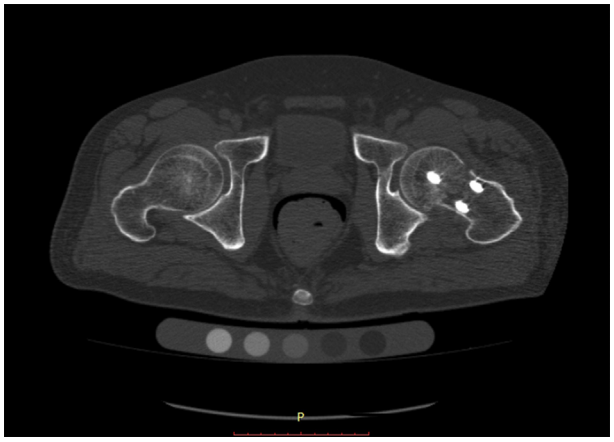

Figure 1 A postoperative computed tomography scan of a hip. The axial slice shows that a cannulated screw was obtained for interscan reproducibility analysis.

BMD assessment

Before BMD calculation, the QCT data had to be preprocessed so that we could extract the proximal femoral structure. The segmentation of contralateral proximal femur structures in a patient with a hip fracture was created using Seg3D software (Center for Integrative Biomedical Computing, University of Utah, Salt Lake City, UT, USA) from QCT image data. To calculate BMD values, we acquired scans with a QCT calibration phantom. In our study, the BMD conversion formula was obtained in two steps. First, 20 samples were scanned using QCT to obtain CT images, and the HU values corresponding to K_2HPO_4 with known density in the model were extrapolated from the image of the calibration phantom. Second, the least squares curve was used to obtain the correlation between the known mineral density and the corresponding HU value of each slice [20]. Using this method, a linear transformation formula that can convert the HU value to BMD in milligrammes per cubic centimetre was obtained by sample data from 20 patients. The formula is as follows:

$$\mathrm{BMD} = a \times \mathrm{H}_B + b$$

where H_B is the bone tissue CT value and a and b represent the slope and intercept of the equation, respectively.

Automatically calculating the vBMD of the nail tract

A cylinder was used to simulate a nail tract in the proximal femur template. To analyze the bone density distribution around the nail tract, we divided the cylinder into three equal parts to obtain the average vBMD. The construction of the nail tract required three main steps: (1) creating a standard nail tract; (2) mapping the space to a standard template; and (3) automatically calculating the average vBMD of the nail tract.

Step 1: creating a standard nail tract

A standard template was chosen by an experienced surgeon in selecting a standard proximal image of the femur. Empirically, two fixed points were manually selected on the template to generate a 3D cylinder to simulate a nail tract in the femoral head. The standard nail tract was constructed as follows: First, we built a cylinder with two fixed points at the circle's centre and with radius of 10 mm; this was based on clinical experience. Second, we determined the length of the cylinder by calculating the distance between the two fixed points. Third, we divided the cylinder into 375 units, with every 125 units composing one part from bottom to top, for a total of three parts, represented by S1, S2 and S3. And, the average vBMD of whole nail tract is represented by S4. The average vBMD of each unit was acquired by calculating the mean of all vBMD values included, and the average vBMD of every part was determined by averaging the 125 units included.

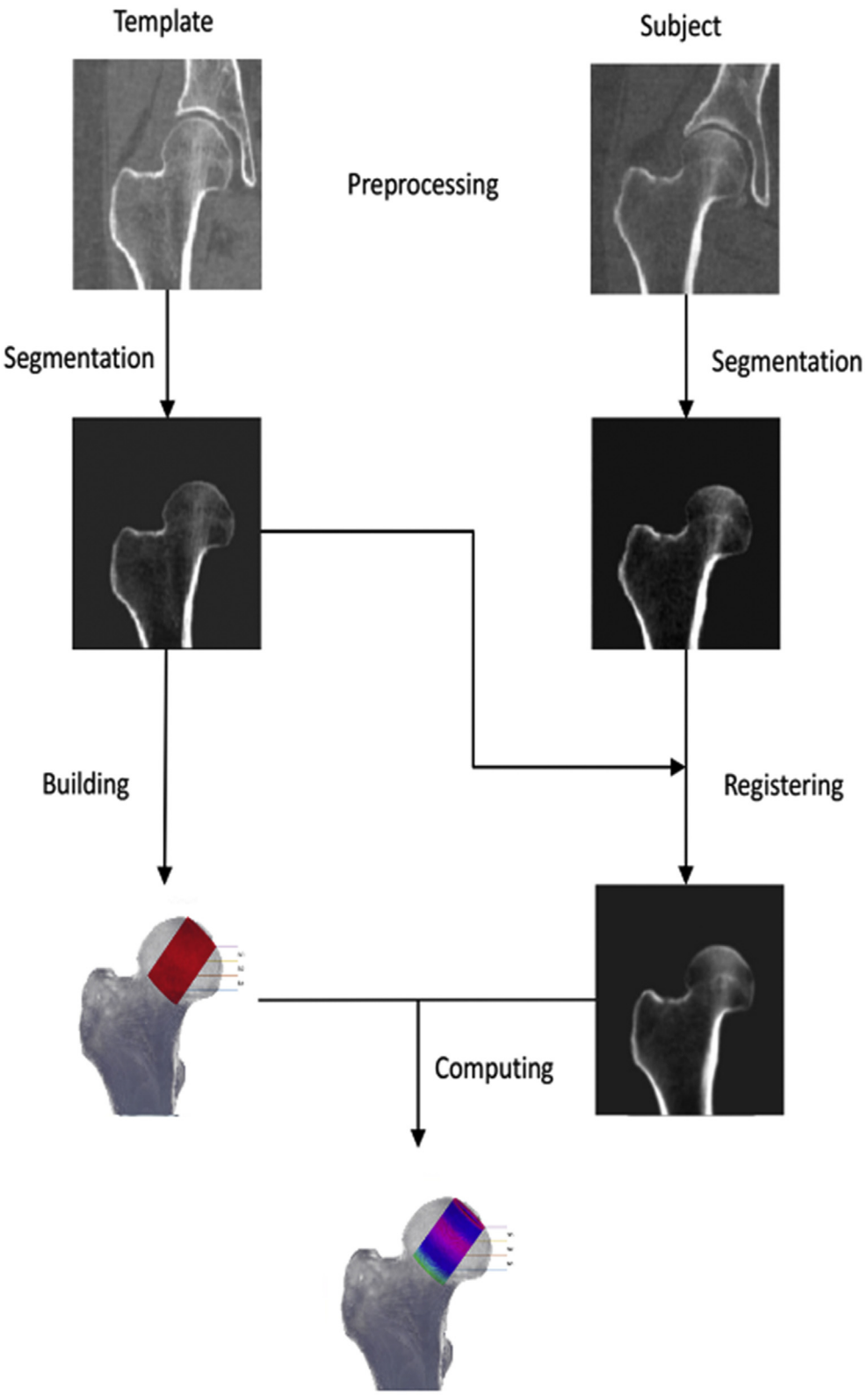

Figure 2 Illustration of the process of calculating the average vBMD of the nail tract. All data are preprocessed, and the proximal femoral structure is segmented from the QCT image. Two fixed points are selected in the template to build a standard nail tract, and the registration algorithm is used to match the patient's femoral structure to the template's femoral structure. The BMD distribution of the registration image was computed by combining Steps 1 and 2 (see the text for an explanation) and then displaying the average vBMD of the nail tract in the three-dimensional space.
BMD = bone mineral density; QCT = quantitative computed tomography; vBMD = volumetric bone mineral density.

Table 1 Characteristics of study participants.

Group	Men/ women	Age (years)	Height (cm)	Weight (kg)
Interscan (n = 26)	6/20	61.6 ± 13.0	163.6 ± 9.1	59.7 ± 12.6
GN (n = 33)	13/20	73.5 ± 14.2	162.0 ± 9.4	62.6 ± 11.5
PFNA (n = 16)	4/12	74.3 ± 9.1	160.1 ± 7.3	62.6 ± 10.1

GN = gamma nail; PFNA = proximal femoral nail antirotation; SD = standard deviation.
Data represent the mean ± SD.

Step 2: mapping the space to a standard template
To determine the proper nail tract for each patient in relation to the standard nail tract in the template, we adopted a two-tier registration method.

In the first tier, a rigid registration was adopted to correct rotation and translation, and then a deformable registration with the free-form B-spline deformation model was implemented to correct heterogeneous deformation [21]. To avoid the distortion of underlying topology caused by the folding of images, we imposed a sufficient condition on the displacements of B-spline control nodes [22], and the L-BFGS-B optimization method was used to minimize the negative of mutual information, which was the objective function [23]. The first-tier registration procedure was implemented using the Insight Segmentation and Registration Toolkit (Kitware, Inc., Clifton Park, NY, USA; https://itk.org/).

In the second tier, we used a tool to further refine the registration results: a diffeomorphic deformable registration algorithm called Advanced Normalization Tools (ANTs; http://stnava.github.io/ANTs/), which is a state-of-the-art deformable registration technique [24].

Step 3: automatically calculating the average vBMD
After a patient was registered to the template, we mapped the patient's proximal femur structure to the template. Therefore, we obtained the position of the patient's nail tract as it corresponded to the standard nail tract in the template. The average vBMD of the patient's nail tract could be obtained by using the standard nail tract. We implemented the method using MATLAB (version 2014a; MathWorks, Natick, MA, USA) and used volume rendering to display the results.

Through these steps, the average vBMD of the nail tract for each patient can be determined (Figure 2).

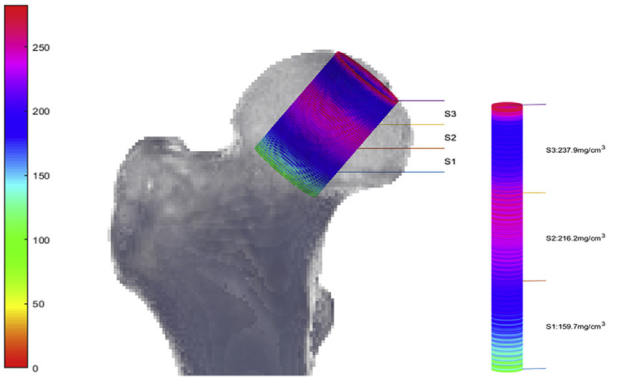

Figure 3 The spatial distribution of average vBMD. The cylinder is used to represent a nail tract. Its resolution is 375 units, and S1, S2 and S3 represent the 3 equal parts of the tract. S4 represents the whole nail tract. To highlight changes in BMD, the colour bar was used to represent the average vBMD for each part; the value is displayed numerically at its corresponding position.
BMD = bone mineral density; vBMD = volumetric bone mineral density.

Statistical analysis

According to the recommendations of the International Society for Clinical Densitometry, the feasibility and reproducibility of the method were evaluated by using the coefficient of variations (CV) of the root mean square of the standard deviation (RMSSD) (CV-RMSSD) [19]. We used the intraoperator group and interscan group for testing. For the intraoperator test, an experienced surgeon manually selected two fixed points on the same sample at two different times and used Step 1 of the method for automatically calculating the average vBMD of the patient's nail tract. For the interscan test, we scanned each patient two times, obtaining two scanned samples, and then we performed the automatic calculation method to determine the average vBMD of the patient's nail tract. The patient's age, height and weight were not considered in the calculation of means, standard deviations, RMSSDs or CV-RMSSDs. In addition, we used this method to analyze the difference between two types of nails, the PFNA and GN. We used the Mann–Whitney U test to compare the average vBMDs for the GN and PFNA tracts. SPSS Statistics software (version 22; IBM, New York, USA) were used for statistical analysis. We used a significance level of 0.05 for all tests.

Table 2 Intraoperator and interscan reproducibility of nail-tract BMD estimation.

Intraoperator reproducibility					Interscan reproducibility			
Site	Operation 1 (n = 29)	Operation 2 (n = 29)	RMSSD	CV-RMSSD	Scan 1 (n = 26)	Scan 2 (n = 26)	RMSSD	CV-RMSSD
S1	128.49 ± 32.72	128.01 ± 32.15	3.7	2.0	149.15 ± 30.17	150.15 ± 29.91	8.7	4.5
S2	141.85 ± 30.66	142.33 ± 31.4	2.8	1.5	202.95 ± 37.17	203.49 ± 36.67	9.7	3.6
S3	136.87 ± 39.74	137.54 ± 40.57	3.7	1.9	212.16 ± 51.05	213.71 ± 49.97	10.5	3.7
S4	135.74 ± 32.34	135.96 ± 32.75	1.8	1.0	188.09 ± 37.76	189.11 ± 37.27	9.2	3.7

BMD = bone mineral density; CV = coefficient of variation; RMSSD = root mean square of the SD; SD = standard deviation.
Data represent the mean ± SD.

Table 3 Intramedullary nail type: average volume BMD and SD of GN and PFNA.

Site	Mean ± SD		*p*
	GN (n = 33)	PFNA (n = 16)	
S1	146.45 ± 38.72	145.09 ± 27.36	0.915
S2	200.47 ± 46.3	203.47 ± 30.69	0.717
S3	191.91 ± 50.88	190.76 ± 31.21	0.685
S4	179.61 ± 43.34	179.77 ± 27.21	0.815

BMD = bone mineral density; GN = gamma nail; PFNA = proximal femoral nail antirotation; SD = standard deviation.

Results

The characteristics of study participants are shown in Table 1. Table 2 shows findings for the intraoperator and interscan groups. For the intraoperator group, the CV-RMSSD ranged from 1.0% to 2.0%, whereas it ranged from 3.6% to 4.5% for the interscan group. The BMD spatial distribution for the nail tract in the contralateral proximal femur is shown in Figure 3, in which pseudocolours represent changes in average vBMD. All data were compared with data for the contralateral proximal femur.

We applied our proposed method to analyze the GN and PFNA, which are used in surgical treatment of fractures (Table 3). The *p* value range for the two groups was 0.685—0.915 ($p > 0.05$). The average vBMD for all patients are shown in Figure 4.

Discussion

Bone quality cannot be evaluated directly *in vivo*; thus, BMD is recognized as a surrogate of bone quality and is highly correlated to bone strength [25,26]. In this study, we successfully established a reliable method in evaluating the BMD of the intramedullary nail tract, and we applied our proposed method to analyze the difference between the PFNA and GN and found no significant difference in average vBMD between the two groups.

Although some studies have indicated that bone quality might be essential for the reconstruction of trochanteric fractures [6,27—29], there has been no accurate and specific measurement tool. Neither DXA nor QCT is an ideal assessment tool. DXA is a two-dimensional technique, and the imaging problem of overlapping femoral head makes bone assessments of such region impossible [30]. Although QCT can provide BMD of trabecular bone of the femoral head, which was not influenced by the bone overlapping around the femoral head, the precision of QCT measurement on femoral head is not good [29]. Previous studies investigated some indirect bone density assessments to examine the relationship of bone density and cut-out failure [31]. For example, Richards et a1 [32] determine the bone density by establishing the compression strength of a plug of bone removed from the femoral neck, and Smith et a1 [33] used the Singh index and a regional BMD computed tomographic protocol to establish bone density. The method we proposed could set up nail tract and estimate the spatial BMD of the femoral head's nail tract. It is documented that a CV-RMSSD

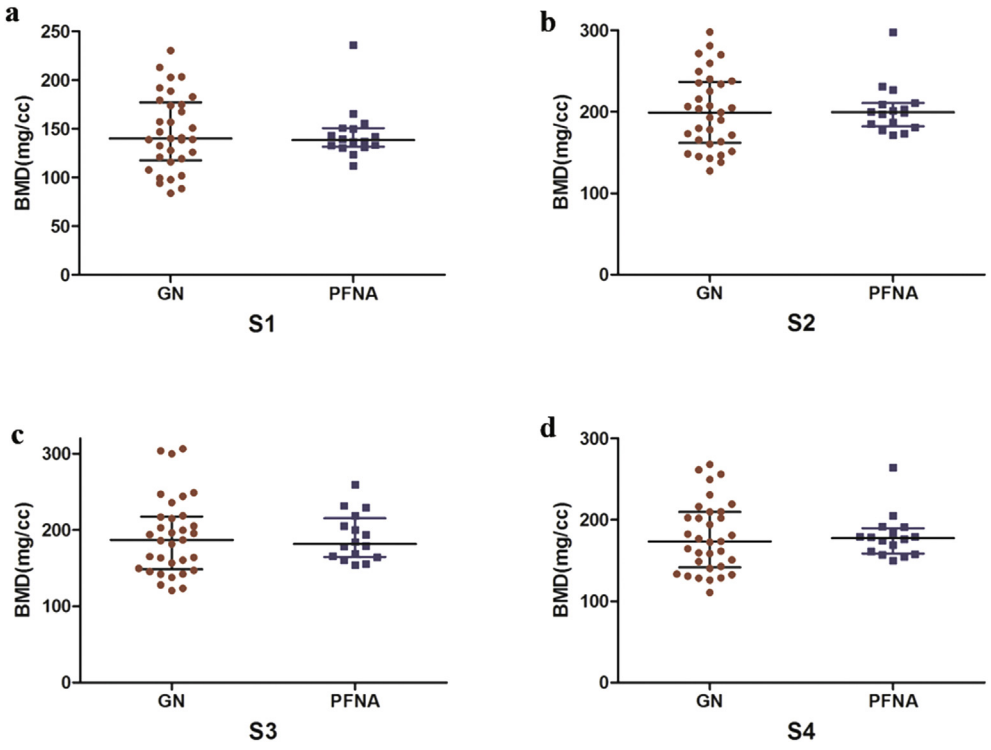

Figure 4 Vertical scatter plots of average vBMD for regions S1 through S4 for the proximal femoral nail antirotation (PFNA) and gamma nail (GN) groups. A—D show the average vBMD distribution of PFNA and GN in S1, S2, S3 and S4 region, respectively. BMD = bone mineral density; vBMD = volumetric bone mineral density.

lower than 10% indicated good reproducibility [34]. Our findings demonstrate the high reproducibility of measurements using the BMD estimation tool with CV-RMSSD lower than 5%. Hence, the results of our study are acceptable and reliable. Several studies indicated that PFNA might be a better device for intertrochanteric fracture, resulting in less blood loss and a lower rate of fixation failure in comparison with the GN [6,35,36]. PFNA is suitable for patients with low bone density in the femoral head, whereas GN is suitable for patients with high bone density in the femoral head. However, the helical blade of the PFNA means less contact surface with the cancellous bone in the axial direction, which means that the nail would be more prone to cut out. A biomechanical study found an axial contact surface of 75 mm^2 for the PFNA blade and 300 mm^2 for the GN [37]. Cut-out is the most common cause of fixation failure with implants. The position of the lag screw within the femoral head is also an important factor in the success or failure of the implant. Our results showed that there are no significant differences in average vBMD distribution between GN group and PFNA groups, which may indicate that the selection of intramedullary nails on the surgeon's experience was biased. In future, assessing nail-tract BMD by our method before surgery may help surgeons to select the appropriate intramedullary nails for specific patients with different nail-tract BMD. However, this hypothesis needs further investigation.

Our study had several limitations. First, we choose 10 mm as the radius of the cylinder after surgeons for their recommendations. However, we found that different radius sizes led to differing average BMD values and that choosing the radius size to better assess the average vBMD of nail tract is worthy of further study. Second, the relationship between BMD and choice of head screw for intramedullary nail fixation remains to be elucidated, so further *in vitro* research is necessary. And also, our study did not examine parameters of crucial importance for the prevention of fixation failure such as the configuration of the fracture, the degree of comminution, the accuracy of reduction and the possibility to insert the head screw at the preplanned position. A necessary next step is to validate it in an appropriately designer clinical trial to provide a useful and practice-changing tool to surgeons for the preoperative planning and fixation of hip fractures.

To our knowledge, we are the first to develop a method for measuring the spatial average vBMD of nail tracts, but our preliminary findings must be validated in clinical practice research. Additional prospective studies using the proposed method to make treatment planning and evaluate the treatment outcome are necessary before the technique can become a common part of clinical practice. Nevertheless, the proposed method has good potentials to provide a reference index for surgeons to choose appropriate implants.

Conflict of interest statement

The authors declare that they have no conflict of interest.

Ethical statement

Institutional Review Board approval was obtained.

Acknowledgments

We thank the radiology department within the emergency department of Beijing Jishuitan Hospital for scanning the samples. This study was supported by grants from the Beijing Bureau of Health 215 program (Grant numbers: 2013-3-033; 2009-2-03), Capital Characteristic Clinic Project (Grant number: Z141107002514072), National Natural Science Foundation of China (Grant number: 81571772).

References

[1] Cummings SR, Melton LJ. Epidemiology and outcomes of osteoporotic fractures. Lancet 2002;359(9319):1761—7.
[2] Abrahamsen B, van Staa T, Ariely R, Olson M, Cooper C. Excess mortality following hip fracture: a systematic epidemiological review. Osteoporos Int 2009;20(10):1633—50.
[3] Panula J, Pihlajamaki H, Mattila VM, Jaatinen P, Vahlberg T, Aarnio P, et al. Mortality and cause of death in hip fracture patients aged 65 or older - a population-based study. BMC Muscoskelet Disord 2011;12:105.
[4] Parker MJ, Handoll HHG. Gamma and other cephalocondylic intramedullary nails versus extramedullary implants for extracapsular hip fractures in adults. Cochrane Database Syst Rev 2010;8(9):CD000093.
[5] Ostrum RF, Tornetta P, Watson JT, Christiano A, Vafek E. Ipsilateral proximal femur and shaft fractures treated with hip screws and a reamed retrograde intramedullary nail. Clin Orthop Relat Res 2014;472(9):2751—8.
[6] Schipper IB, Marti RK, van der Werken C. Unstable trochanteric femoral fractures: extramedullary or intramedullary fixation - review of literature. Injury Int J Care Injured 2004; 35(2):142—51.
[7] Chinzei N, Hiranaka T, Niikura T, Tsuji M, Kuroda R, Doita M, et al. Comparison of the sliding and femoral head rotation among three different femoral head fixation devices for trochanteric fractures. Clin Orthop Surg 2015;7(3):291—7.
[8] Bergkvist G, Koh KJ, Sahlholm S, Klintstrom E, Lindh C. Bone density at implant sites and its relationship to assessment of bone quality and treatment outcome. Int J Oral Maxillofac Implants 2010;25(2):321—8.
[9] Blake GM, Fogelman I. The role of DXA bone density scans in the diagnosis and treatment of osteoporosis. Postgrad Med 2007;83(982):509—17.
[10] Cheng XG, Wang L, Wang QQ, Ma YM, Su YB, Li K. Validation of quantitative computed tomography-derived areal bone mineral density with dual energy X-ray absorptiometry in an elderly Chinese population. Chinese Med J Peking 2014;127(8):1445—9.
[11] Engelke K, Libanati C, Liu Y, Wang H, Austin M, Fuerst T, et al. Quantitative computed tomography (QCT) of the forearm using general purpose spiral whole-body CT scanners: accuracy, precision and comparison with dual-energy X-ray absorptiometry (DXA). Bone 2009;45(1):110—8.
[12] Bredbenner TL, Mason RL, Havill LM, Orwoll ES, Nicolella DP, MrOS OFM. Fracture risk predictions based on statistical shape and density modeling of the proximal femur. J Bone Miner Res 2014;29(9):2090—100.
[13] Carballido-Gamio J, Bonaretti S, Saeed I, Harnish R, Recker R, Burghardt AJ, et al. Automatic multi-parametric quantification of the proximal femur with quantitative computed tomography. Quant Imag Med Surg 2015;5(4):552—68.
[14] Carballido-Gamio J, Harnish R, Saeed I, Streeper T, Sigurdsson S, Amin S, et al. Proximal femoral density distribution and structure in relation to age and hip fracture risk in women. J Bone Miner Res 2013;28(3):537—46.

[15] Li WJ, Kornak J, Harris TB, Keyak J, Li CX, Lu Y, et al. Bone fracture risk estimation based on image similarity. Bone 2009; 45(3):560—7.
[16] Sarkalkan N, Weinans H, Zadpoor AA. Statistical shape and appearance models of bones. Bone 2014;60:129—40.
[17] Yu AH, Carballido-Gamio J, Wang L, Lang TF, Su YB, Wu XB, et al. Spatial differences in the distribution of bone between femoral neck and trochanteric fractures. J Bone Miner Res 2017;32(8):1672—80.
[18] Cheng X, Li J, Lu Y, Keyak J, Lang T. Proximal femoral density and geometry measurements by quantitative computed tomography: association with hip fracture. Bone 2007;40(1): 169—74.
[19] Gluer CC, Blake G, Lu Y, Blunt BA, Jergas M, Genant HK. Accurate assessment of precision errors — how to measure the reproducibility of bone densitometry techniques. Osteoporos Int 1995;5(4):262—70.
[20] Emami A, Ghadiri H, Ghafarian P. Performance evaluation of bone mineral densitometry techniques by a novel phantom. Front Biomed Technol 2014;1(4):271—8.
[21] Xia W, Gao X. A fast deformable registration method for 4D lung CT in hybrid framework. Int J Comput Assist Radiol Surg 2014;9(4):523—33.
[22] Choi Y, Lee S. Injectivity conditions of 2D and 3D uniform cubic B-spline functions. Graph Model 2000;62(6):411—27.
[23] Zhu CY, Byrd RH, Lu PH, Nocedal J. Algorithm 778: L-BFGS-B: fortran subroutines for large-scale bound-constrained optimization. Acm T Math Software 1997;23(4):550—60.
[24] Avants BB, Epstein CL, Grossman M, Gee JC. Symmetric diffeomorphic image registration with cross-correlation: evaluating automated labeling of elderly and neurodegenerative brain. Med Image Anal 2008;12(1):26—41.
[25] Cheng XG, Lowet G, Boonen S, Nicholson PHF, Brys P, Nijs J, et al. Assessment of the strength of proximal femur in vitro: relationship to femoral bone mineral density and femoral geometry. Bone 1997;20(3):213—8.
[26] Lang TF, Keyak JH, Heitz MW, Augat P, Lu Y, Mathur A, et al. Volumetric quantitative computed tomography of the proximal femur: precision and relation to bone strength. Bone 1997;21(1):101—8.
[27] Babhulkar S. Unstable trochanteric fractures: issues and avoiding pitfalls. Injury Int J Care Injured 2017;48(4):803—18.
[28] Lindskog DM, Baumgaertner MR. Unstable intertrochanteric hip fractures in the elderly. J Am Acad Orthop Sur 2004;12(3): 179—90.
[29] Yi C, Wang MY, Wei J, Wang J, Wang L, Cheng XG. Preoperative QCT assessment of femoral head for assessment of femoral head bone loss. Exp Ther Med 2017;13(4):1470—4.
[30] Engelke K. Quantitative computed tomography-current status and new developments. J Clin Densitom 2017;20(3): 309—21.
[31] Babhulkar S. Unstable trochanteric fractures: issues and avoiding pitfalls. Injury 2017;48(4):803—18.
[32] Richards RH, Evans G, Egan J, Shearer JR. The AO dynamic hip screw and the Pugh sliding nail in femoral head fixation. J Bone Joint Surg Br Vol 1990;72(5):794—6.
[33] Smith MD, Cody DD, Goldstein SA, Cooperman AM, Matthews LS, Flynn MJ. Proximal femoral bone density and its correlation to fracture load and hip-screw penetration load. Clin Orthop Relat Res 1992;(283):244—51.
[34] Chaplais E, Greene D, Hood A, Telfer S, du Toit V, Singh-Grewal D, et al. Reproducibility of a peripheral quantitative computed tomography scan protocol to measure the material properties of the second metatarsal. BMC Muscoskelet Disord 2014;15:242.
[35] Ma KL, Wang X, Luan FJ, Xu HT, Fang Y, Min J, et al. Proximal femoral nails antirotation, Gamma nails, and dynamic hip screws for fixation of intertrochanteric fractures of femur: a meta-analysis. Orthop Traumatol Sur 2014;100(8): 859—66.
[36] Simmermacher RKJ, Ljungqvist J, Bail H, Hockertz T, Vochteloo AJH, Ochs U, et al. The new proximal femoral nail antirotation (PFNA (R)) in daily practice: results of a multicentre clinical study. Injury Int J Care Injured 2008;39(8): 932—9.
[37] Born CT, Karich B, Bauer C, von Oldenburg G, Augat P. Hip screw migration testing: first results for hip screws and helical blades utilizing a new oscillating test method. J Orthop Res Off Publ Orthop Res Soc 2011;29(5):760—6.